Geol. Mag.: page 1 of 9 © Cambridge University Press 2017
doi:10.1017/S0016756816001175

A new SIMS zircon U–Pb date from the Ediacaran Doushantuo Formation: age constraint on the Weng'an biota

CHUANMING ZHOU*†, XIAN-HUA LI‡, SHUHAI XIAO§, ZHONGWU LAN‡, QING OUYANG*¶, CHENGGUO GUAN* & ZHE CHEN*

*CAS Key Laboratory of Economic Stratigraphy and Palaeogeography, Nanjing Institute of Geology and Palaeontology, Chinese Academy of Sciences, Nanjing 210008, China
‡State Key Laboratory of Lithospheric Evolution, Institute of Geology and Geophysics, Chinese Academy of Sciences, Beijing 100029, China
§Department of Geosciences, Virginia Tech, Blacksburg, VA 24061, USA
¶University of Chinese Academy of Sciences, Beijing 100049, China

(*Received* 26 July 2016; *accepted* 30 November 2016)

Abstract – As a well-known phosphatized Lagerstätte, the Ediacaran Weng'an biota in central Guizhou Province of South China contains diverse acanthomorphic acritarchs, algal thalli, tubular microfossils as well as various spheroidal fossils. These fossils provide crucial palaeontological evidence for the radiation of multicellular eukaryotes after the termination of the Neoproterozoic global glaciation. While the Weng'an biota is generally considered as early Ediacaran in age on the basis of phosphorite Pb–Pb isochron ages ranging from 572 Ma to 599 Ma, the reliability and accuracy of these age data have been questioned and some geologists have proposed that the Weng'an biota may be younger than 580 Ma instead. Here we report a SIMS zircon U–Pb age of 609 ± 5 Ma for a tuffaceous bed immediately above the upper phosphorite unit in the Doushantuo Formation at Zhangcunping, Yichang, South China. Litho-, bio- and chemostratigraphic correlations suggest that the upper phosphorite unit at Zhangcunping can be well correlated with the upper phosphorite unit at Weng'an, which is the main horizon of the Weng'an biota. We therefore conclude that the Weng'an biota could be as old as 609 ± 5 Ma.

Keywords: phosphatized Lagerstätte, lithostratigraphic and biostratigraphic correlation, tuffaceous bed, Zhangcunping, South China

1. Introduction

The rise of multicellularity represents a major evolutionary transition (Maynard Smith & Szathmary, 1998). Multicellular eukaryotes may have evolved as early as during Palaeoproterozoic time, but their diversity remains relatively low until the Ediacaran Period (Knoll *et al.* 2006; Xiao *et al.* 2014*a*). The Ediacaran Period is characterized by a series of exceptionally preserved fossil Lagerstätten, including the Lantian biota (Yuan *et al.* 2011), Weng'an biota (Xiao *et al.* 2014*a*; Yuan *et al.* 2002) and Miaohe biota (Ding *et al.* 1996; Xiao *et al.* 2002), as well as the Avalon assemblage (Narbonne, 2004), White Sea assemblage (Martin *et al.* 2000) and Nama assemblage (Grotzinger *et al.* 1995) of the Ediacara biota. Among these Ediacaran biotas, the Weng'an biota in the Doushantuo Formation of central Guizhou Province of South China stands out for its extraordinary fossil preservation at cellular and subcellular levels (Hagadorn *et al.* 2006; Xiao, Zhang & Knoll, 1998). It provides a unique window to explore the early evolution of cellularly differentiated eukaryotes, including multicellular algae and animals (Chen *et al.* 2014*a*; Xiao *et al.* 2014*a*).

†Author for correspondence: cmzhou@nigpas.ac.cn

The stratigraphic background of the Weng'an biota has been published previously (Xiao *et al.*, 2014*a*) and is briefly summarized here. The Doushantuo Formation at Weng'an (Fig. 1) overlies the Cryogenian Nantuo Formation and underlies the terminal Ediacaran Dengying Formation (Fig. 2). It begins with a cap dolostone (unit 1) that is widely distributed and easily recognizable in South China. The cap carbonate is followed by unit 2 or lower phosphorite that is characterized by thin-bedded, peloidal phosphorite with interbedded dolostone. Unit 3 is a 2–4 m thick massive dolostone, also known as the mid-Doushantuo dolostone, with a prominent karstification surface on top. Further upsection, unit 4 or upper phosphorite consists of 3–10 m thick intraclastic phosphorite; this unit is further divided into the lower unit 4A (black facies) and the upper unit 4B (grey facies). Unit 5 is *c.* 10 m thick phosphatic dolostone, which may contain an additional exposure surface. The Weng'an biota occurs in units 4–5, but the main repository is in unit 4A (black facies) and 4B (grey facies).

Despite the key role it plays in the study of Ediacaran palaeobiology, the Weng'an biota is poorly constrained by radiometric ages. Previously published radiometric dates from the Doushantuo Formation at Weng'an include whole-rock Pb–Pb isochron ages of

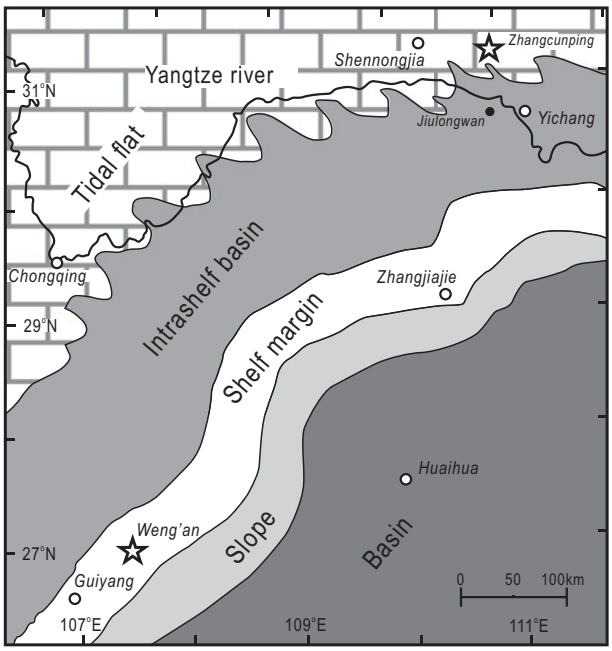

Figure 1. Palaeogeographic reconstruction of the Ediacaran Doushantuo Formation (Jiang *et al.* 2011) and locations of the studied Zhangcunping and Weng'an sections (stars).

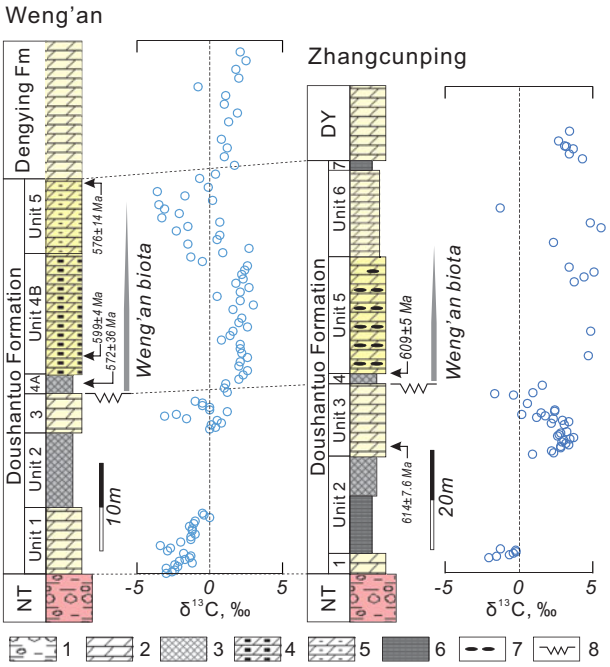

Figure 2. (Colour online) Litho-, chemo- and biostratigrasphic correlation of the Doushantuo Formation at Zhangcunping and Weng'an. Radiometric dates are from Barfod *et al.* (2002), Chen *et al.* (2004), Chen *et al.* (2009) and this study. $\delta^{13}C$ data are from Zhou *et al.* (2007) for Weng'an section and Yuan *et al.* (2011) for Zhangcunping section. 1, diamictite; 2, dolostone; 3, phosphorite; 4, dolomitic phosphorite; 5, phosphatic dolostone; 6, black shale; 7, chert/phosphatic nodules; 8, erosional surface. NT – Nantuo Formation; DY – Dengying Formation.

572 ± 36 Ma (Chen *et al.* 2009), 599 ± 4 Ma (Barfod *et al.* 2002) and 576 ± 14 Ma (Chen *et al.* 2004) from units 4A, 4B and 5, respectively. Although these ages are consistent within errors with each other and suggest that the Weng'an biota is *c.* 600 Ma, they have large error bars and are considered unreliable (Condon *et al.* 2005). Instead, Condon *et al.* (2005) proposed that the Weng'an biota is younger than *c.* 580 Ma based on the assumption that the exposure surface atop unit 3 represents a sedimentary response to the *c.* 582 Ma Gaskiers glaciation.

The poor age constraint on the Weng'an biota hampers our understanding of the evolutionary pattern of Ediacaran marine ecosystems. For example, it has traditionally been believed that the marine ecosystems during early Ediacaran time (635–580 Ma) is dominated by microscopic eukaryotes, including spiny acritarchs and spheroidal fossils in the Weng'an biota, with macro-organisms (e.g. those in the Lantian biota; Wan *et al.* 2016) playing a subordinate role; the late Ediacaran (580–541 Ma) marine ecosystems are however characterized by the ecological dominance of macro-organisms including the Ediacara biota (e.g. Xiao & Laflamme, 2008). If the Weng'an biota is younger than 580 Ma as suggested by Condon *et al.* (2005), then it is possible for the Weng'an biota to temporally overlap with the Ediacara biota.

The Doushantuo Formation at Zhangcunping in Yichang of western Hubei Province, South China, exhibits lithostratigraphic sequence and yields phosphatic fossil assemblage similar to those at Weng'an (Chen *et al.* 2010; McFadden *et al.* 2009; Ye *et al.* 2015; Zhou, Xie & Xiao, 2005). The Zhangcunping section can therefore provide an independent test of the age of the Weng'an biota. In this paper, we report a SIMS zircon U–Pb age from a tuffaceous bed immediately above the upper phosphorite unit at Zhangcunping, which is correlated with unit 4 at Weng'an.

2. Geological setting and sample horizon

Facies analyses of representative sections on the Yangtze Block suggest that the basal Doushantuo Formation was deposited in an open shelf setting, which then evolved into a rimmed shelf shortly after the deposition of the Doushantuo cap dolostone (Jiang *et al.* 2011). The Zhangcunping section is located in the inner shelf whereas the Weng'an section in located in the outer shelf, both in shallow-water environments (Fig. 1) (Cao *et al.* 1989; Jiang *et al.* 2011). Facies variation is expected in both sites because of the exposure of the shallow-water carbonate platform and facies migration towards the shelf lagoon (Jiang *et al.* 2011).

The lithostratigraphic sequence of the Doushantuo Formation at Zhangcunping resembles that at Weng'an (Fig. 2). The Doushantuo Formation (*c.* 90 m in thickness) generally consists of seven units, though the thickness of each unit varies in this area. Overlying the Cryogenian Nantuo Formation diamictite, the Ediacaran Doushantuo Formation begins with *c.* 3 m of the cap dolostone (unit 1) followed by 2–24 m of black shale with phosphorite and dolostone interbeds

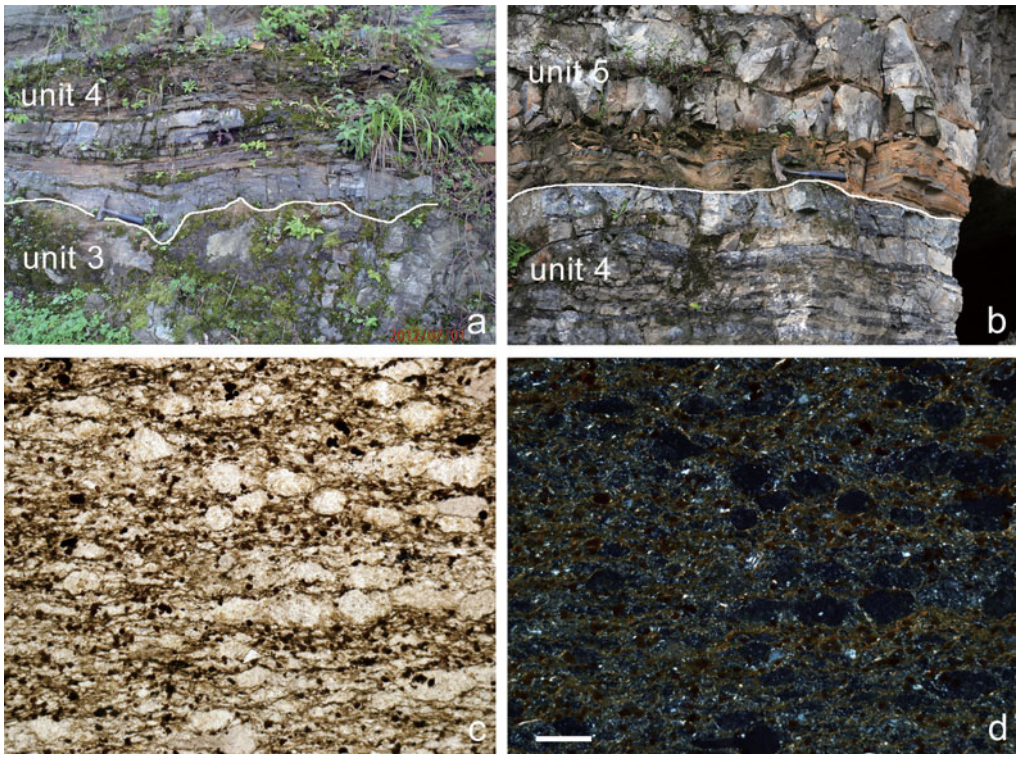

Figure 3. (Colour online) Outcrop and thin-section photographs: (a) unit 4 phosphorite deposited on the erosional surface at the top of unit 3 dolostone; (b) brown tuffaceous bed immediately overlies the unit 4 phosphorite; (c, d), thin-section photographs taken under plane and polarized transmitted light, respectively, showing phosphatic/chert nodules within tuffaceous silty and argillaceous matrix. Hammers in (a) and (b) are *c.* 30 cm long, scale bar in (d) 100 μm, also applicable to (c).

(unit 2). The phosphotite unit is overlain by 4–20 m of medium-bedded dolostone (unit 3), with an erosional surface at the top (Fig. 3a) and a 614.0 ± 7.6 Ma ash bed at the base (Liu *et al.* 2009). Overlying the erosional surface, unit 4 is characterized by the 5–12 m of phosphorite interbedded with dolostone (Fig. 3a, b). The succeeding unit 5 begins with a 30 cm thick tuffaceous siltstone and mudstone (Figs 2, 3b), followed by *c.* 30 m of greyish-black thin- to medium-bedded dolostones with abundant cherty and phosphatic nodules and thin layers. Unit 6 is >20 m thick and consists of thin-bedded dolostone, which is overlain by unit 7 of 1–2 m black shale. The Doushantuo Formation is overlain by the Dengying Formation dolostone. Phosphatized multicellular algal fossils and acanthomorphic acritarchs taxonomically similar to those in the Weng'an biota have been reported from units 4 and 5 (Fig. 4; Chen *et al.* 2010; Liu *et al.* 2009; McFadden *et al.* 2009; Ye *et al.* 2015; Zhou, Xie & Xiao, 2005).

The tuffaceous bed occurs in unit 5 at Lizhi road-cut section (31° 19.944′ N, 111° 12.361′ E). In contrast to adjacent grey dolostone and dark grey phosphorite, it is brown in colour on weathered outcrop and contains centimetre-thick phosphorite/chert layers (Fig. 3b). Thin-section observation under microscope indicates that these layers consist of phosphorite/chert nodules within tuffaceous silty and argillaceous matrix (Fig. 3c, d).

3. SIMS zircon U–Pb analytical procedures

Zircon concentrates were separated from a *c.* 10 kg of tuffaceous sample (sample number 15LZash1) using standard density and magnetic separation techniques. Zircon grains, together with zircon standard Plešovice 91500 and Qinghu, were mounted in an epoxy disc, which was then polished to expose the zircon crystals for analysis. All zircons were documented with transmitted and reflected light photomicrographs and cathodoluminescence (CL) images to reveal their internal structures. The mount was cleaned and vacuum-coated with high-purity gold prior to SIMS analysis.

Measurements of U, Th and Pb isotopes were conducted using a Cameca IMS 1280HR large-radius SIMS at the Institute of Geology and Geophysics, Chinese Academy of Sciences in Beijing. Analytical procedures are the same as those described by Li *et al.* (2009). The O_2^- primary ion beam was accelerated at 13 kV, with an intensity of *c.* 8 nA. The aperture illumination mode (Kohler illumination) was used with a 200 μm primary beam mass filter (PBMF) aperture to produce even sputtering over the entire analysed area. The ellipsoidal spot is about 20×30 μm in size. Positive secondary ions were extracted with a 10 kV potential. The 'oxygen flooding technique' with a working O_2 gas pressure of *c.* 5×10^{-6} Torr (Li *et al.* 2010) was used to enhance the secondary Pb^+ sensitivity to a value of *c.* 38 cps (nA ppm)$^{-1}$ for zircon. In the

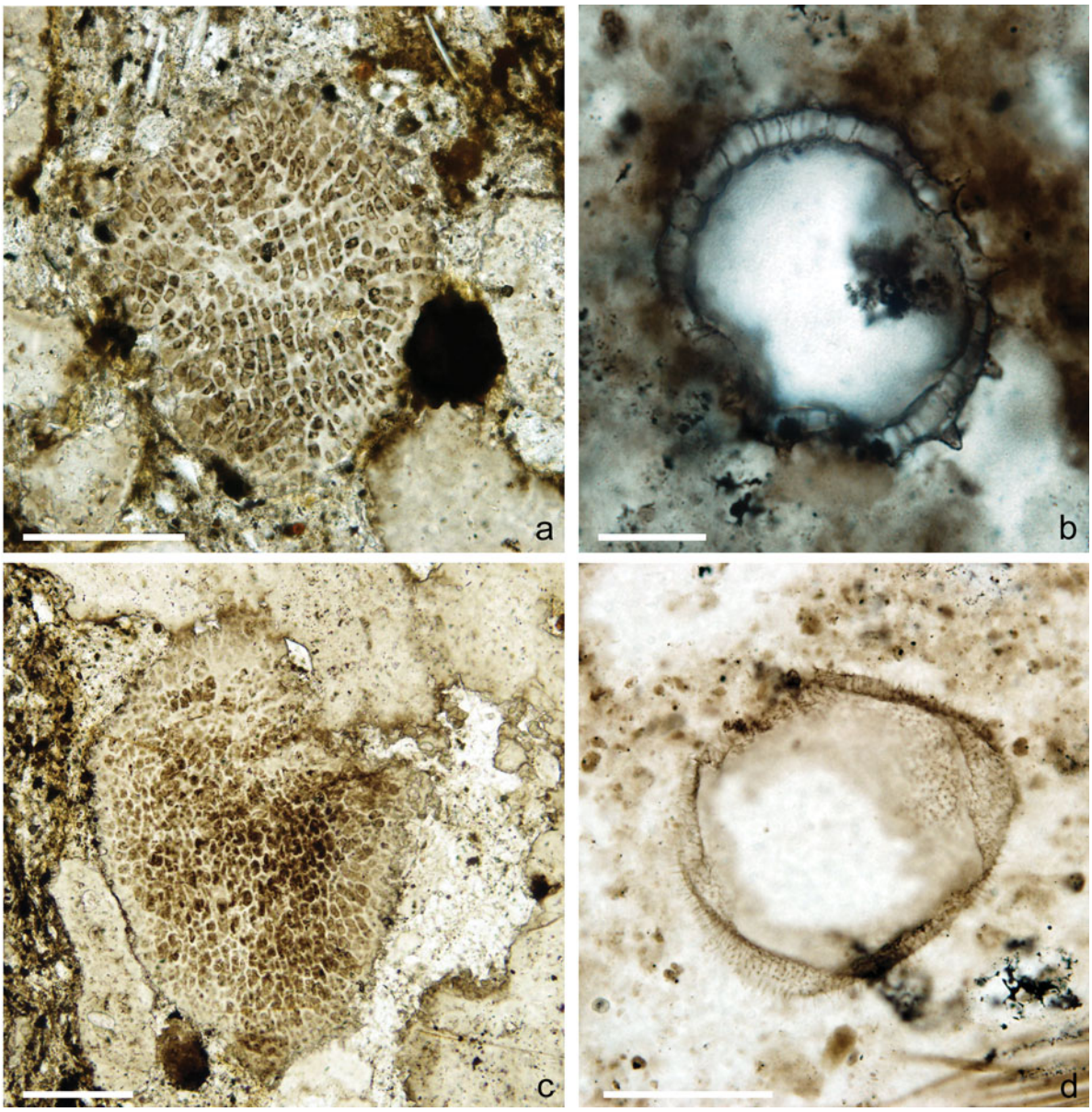

Figure 4. (Colour online) Microfossils from units 4 and 5 of the Doushantuo Formation at Zhangcunping. (a, c) *Wenganian globosa*, 14ZCP-34; (b) *Distosphaera speciosa*, 14ZCP-45; (d) *Knollisphaeridium triangulum*, 14ZCP-46. Scale bars 100 μm in (a, c, d) and 20 μm in (b).

secondary ion beam optics, a 60 eV energy window was used. Mass resolving power is set at 5400 (10 % peak height definition) to separate Pb^+ peaks from isobaric interferences. A single electron multiplier was used in ion-counting mode to measure secondary ion beam intensities by peak jumping.

Pb/U fractionation was calibrated with the power relationship between $^{206}Pb/^{238}U$ and $^{238}U^{16}O2/^{238}U$ against zircon standard Plešovice (Sláma *et al.* 2008); calibration of U and Th abundance was performed relative to zircon standard 91500 (Wiedenbeck *et al.* 1995). A long-term uncertainty of 1.5 % (1 RSD) for $^{206}Pb/^{238}U$ measurements of the standard zircons (Li *et al.* 2010) was propagated to the unknowns, despite the fact that the measured $^{206}Pb/^{238}U$ error during the course of this work is <1 %. Measured compositions were corrected for common Pb using non-radiogenic ^{204}Pb. Corrections are sufficiently small to be insensitive to the choice of common Pb composition, and an average of present-day crustal composition (Stacey & Kramers, 1975) is used for the common Pb assuming that the common Pb is largely surface contamination introduced during sample preparation. Analytical results are listed in Table 1 and uncertainties for individual isotopic data analyses are reported as 1σ. Mean ages for pooled U/Pb analyses are quoted with 95 % confidence interval. Data processing was carried out using the Isoplot 3.70 program (Ludwig, 2008).

In order to ascertain the veracity of SIMS U–Pb measurements calibrated against Plešovice standard, Qinghu zircon standard was alternately analysed as an unknown together with 15LZash1 zircons. Seven measurements conducted on Qinghu yield a Concordia Age of 160.3 ± 1.8 Ma, identical within

Table 1. Geochronological data of the tuffaceous sample 15LZash1.

					Radiogenic isotopic ratios						Isotopic ages					
Spot no.	[U] ppm	[Th] ppm	Th/U	f_{206} (%)	$^{207}Pb/^{235}U$	$\pm\sigma$ (%)	$^{206}Pb/^{238}U$	$\pm\sigma$ (%)	$^{207}Pb/^{206}Pb$	$\pm\sigma$ (%)	$^{207}Pb/^{206}Pb$	$\pm\sigma$	$^{207}Pb/^{235}U$	$\pm\sigma$	$^{206}Pb/^{238}U$	$\pm\sigma$
Group 1																
#01	96	154	1.59	0.11	5.059	1.65	0.3247	1.52	0.1130	0.64	1848.2	11.5	1829.3	14.1	1812.8	24.1
#03	281	143	0.51	0.08	5.132	1.56	0.3258	1.50	0.1142	0.44	1867.8	7.9	1841.4	13.4	1818.2	23.8
#05	603	379	0.63	0.96	1.137	1.88	0.1279	1.52	0.0645	1.11	757.8	23.3	771.2	10.2	775.8	11.1
#08	345	371	1.08	0.54	1.099	1.71	0.1242	1.51	0.0642	0.82	746.6	17.2	752.9	9.2	755.0	10.7
#09	362	141	0.39	0.20	1.169	1.63	0.1292	1.51	0.0656	0.61	793.6	12.7	786.1	9.0	783.4	11.2
#12	318	559	1.76	0.12	1.112	2.42	0.1244	1.51	0.0648	1.89	769.0	39.3	759.1	13.0	755.8	10.8
#17	268	267	1.00	0.72	1.200	2.03	0.1288	1.50	0.0676	1.37	855.2	28.3	800.5	11.3	781.0	11.0
#18	251	313	1.25	0.14	1.040	1.67	0.1170	1.50	0.0645	0.73	756.6	15.3	723.7	8.7	713.2	10.2
Group 2																
#02	162	149	0.92	0.27	0.803	1.96	0.0974	1.50	0.0598	1.26	595.5	27.2	598.3	8.9	599.1	8.6
#04	63	52	0.83	0.24	0.807	2.38	0.0976	1.51	0.0600	1.84	603.5	39.3	600.8	10.9	600.1	8.7
#06	99	145	1.46	0.19	0.834	1.88	0.1002	1.50	0.0604	1.12	616.4	24.1	615.9	8.7	615.7	8.8
#07	33	35	1.05	0.83	0.770	4.47	0.0979	1.62	0.0571	4.16	494.7	89.2	579.8	19.9	601.8	9.3
#10	309	370	1.20	0.43	0.836	1.71	0.1010	1.50	0.0600	0.82	605.3	17.7	616.9	7.9	620.1	8.9
#11	58	50	0.86	0.28	0.810	2.79	0.0990	1.51	0.0594	2.35	580.8	50.2	602.7	12.8	608.5	8.8
#13	160	182	1.13	0.95	0.813	2.75	0.0982	1.50	0.0600	2.30	604.7	49.1	604.1	12.6	604.0	8.7
#14	100	169	1.69	0.21	0.823	2.30	0.0988	1.51	0.0604	1.73	619.1	37.0	609.9	10.6	607.5	8.8
#15	192	200	1.05	0.96	0.817	3.83	0.0986	1.50	0.0601	3.52	607.0	74.4	606.3	17.6	606.2	8.7
#16	111	68	0.61	0.46	0.831	2.04	0.1003	1.53	0.0601	1.35	608.0	28.9	614.2	9.4	615.9	9.0
#19	107	124	1.16	0.92	0.802	2.98	0.0995	1.51	0.0585	2.57	548.4	55.1	598.2	13.6	611.4	8.8
#20	120	120	1.00	0.42	0.851	1.83	0.0999	1.54	0.0618	0.98	668.1	20.8	625.3	8.6	613.6	9.0
#21	236	223	0.95	0.14	0.833	1.73	0.1002	1.51	0.0603	0.85	614.5	18.3	615.3	8.0	615.6	8.9

$^{207}Pb/^{235}U$, $^{206}Pb/^{238}U$ and $^{207}Pb/^{206}Pb$ are common Pb-corrected ratios; f_{206} value is the proportion of common ^{206}Pb in total measured ^{206}Pb.

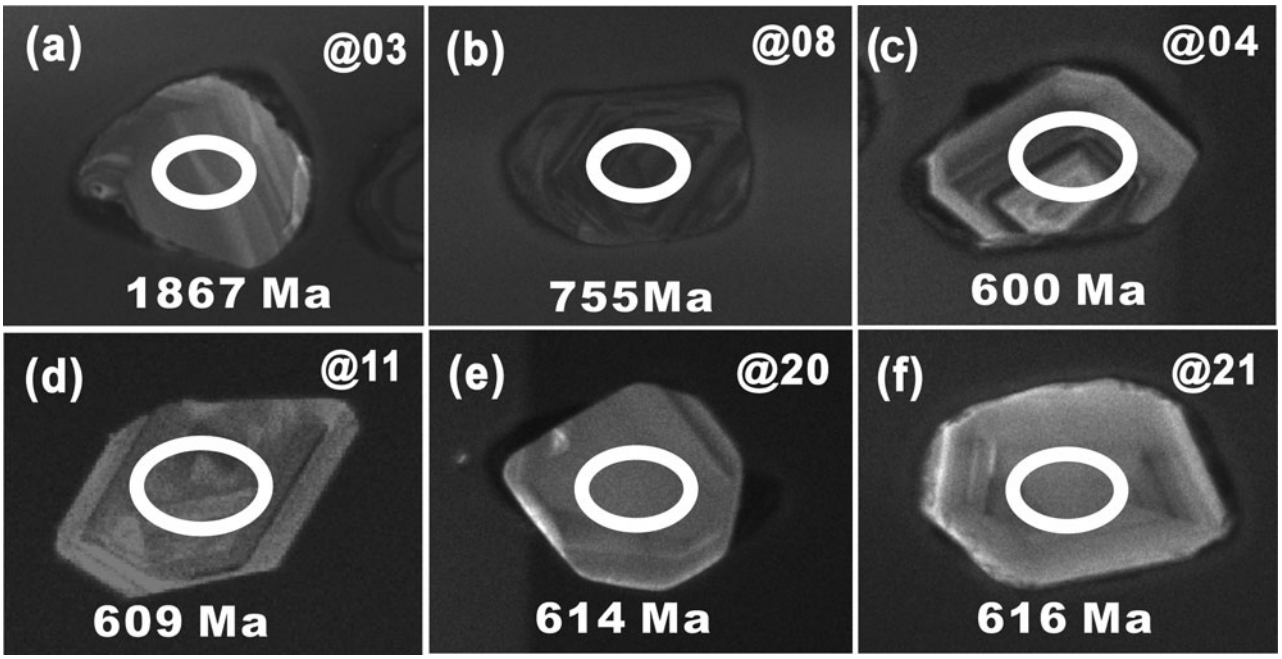

Figure 5. Cathodoluminescence (CL) images for representative zircons from the tuffaceous sample 15LZash1. The ellipses on zircons represent the spots of SIMS U–Pb isotope analyses. SIMS spots are 30 μm in length for scale.

errors to the recommended value of 159.5 ± 0.2 Ma (Li *et al.* 2013).

4. Results

Zircon crystals from the tuff sample 15LZash1 are small in size, 50–100 μm in length and have aspect ratios of 1:1 to 2:1. They can generally be subdivided into two groups in terms of their morphology and CL image features. Group 1 zircons are mostly oval in shape (Fig. 5a, b), whereas group 2 zircons are euhedral to subhedral in shape, showing oscillatory zoning under CL (Fig. 5c–f). Twenty-one analyses were conducted on 21 zircons (Table 1), with 8 and 13 measurements for group 1 and group 2, respectively. Six of eight group 1 zircons are dated at *c.* 750–800 Ma, and the remaining two zircons yield a much older, Palaeoproterozoic age of *c.* 1.85–1.87 Ga (Table 1; Fig. 6). Considering their oval shape and scattered ages, they are most likely xenocrysts. Such Neoproterozoic and Palaeoproterozoic zircons are common in the Yangtze Block (e.g. Liu *et al.* 2008). The group 2 zircons have U concentrations ranging over 33–309 ppm, Th concentrations over 35–370 ppm and Th/U ratios over 0.61–1.69. Common Pb is low, and values of f_{206} are all <1 %. All analyses have concordant U–Pb ages within analytical errors (Fig. 6), yielding a U–Pb Concordia age of 609 ± 5 Ma (MSWD of concordance = 0.34), which is interpreted as the best estimate of the crystallization age of group 2 zircons in the tuff sample 15LZash1. This age therefore provides an estimate of the depositional age of basal unit 5 and, together with the 614.0 ± 7.6 Ma age from unit 3 (Liu *et al.* 2009), it provides an age constraint on the phosphatized fossil assemblage occurring at Zhangcunping and therefore the Weng'an biota that occurs in unit 4 of the Doushantuo Formation at Weng'an through correlation.

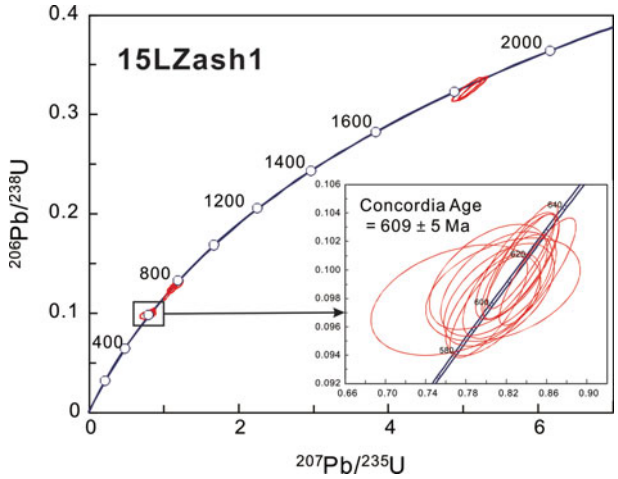

Figure 6. (Colour online) SIMS zircon U–Pb concordia age plot for the tuffaceous sample 15LZash1.

5. Age constraint on the Weng'an biota

Lithostratigraphic sequences of the Doushantuo Formation at Zhangcunping and Weng'an can be easily correlated (Fig. 2; Zhou, Xie & Xiao, 2005). In particular, the erosional surface atop unit 3 (middle dolostone) at both Zhangcunping and Weng'an sections represents a regional subaerial exposure and karstification event in shallow-water carbonate facies including the inner- and outer-shelf shoal complex, with deeper-water facies (such as the shelf basin Jiulongwan section) unaffected. The lithostratigraphic correlation is strongly supported by the biostratigraphic

data obtained from the Zhangcunping (Chen *et al.* 2010; Liu *et al.* 2009; McFadden *et al.* 2009; Ye *et al.* 2015; Zhou, Xie & Xiao, 2005) and Weng'an sections (e.g. Xiao *et al.* 2014*b*), with taxonomically similar multicellular algae, spheroidal fossils and acanthomorphic acritarchs occurring in phosphorite in units 4–5 at both sections. The $\delta^{13}C$ profiles of the Doushantuo Formation at Zhangcunping and Weng'an also show similar chemostratigraphic trends, further supporting the litho- and biostratigraphic correlations (Fig. 2).

Accepting the aforementioned stratigraphic correlation, the 609 ± 5 Ma age from basal unit 5 at Zhangcunping also represents the depositional age of unit 4 at Weng'an, providing an age constraint on the Weng'an biota. The Weng'an biota therefore first appeared no later than 609 ± 5 Ma.

The new age also suggests that the karstic surface atop unit 3 at both Weng'an and Zhangcunping must be >609 ± 5 Ma and therefore cannot be a glacio-eustatic response to the 582 Ma Gaskiers glaciation as proposed previously (Condon *et al.* 2005). Furthermore, the Weng'an biota must pre-date both the 582 Ma Gaskiers glaciation and the 575–565 Ma Avalon assemblage. It remains to be shown whether elements of the Weng'an biota, particularly some acanthomorphic acritarchs, may extend to younger strata and overlap with the Ediacara biota of macroscopic organisms (Xiao *et al.* 2014*b*), but it is clear that microscopic fossils of the Weng'an biota appeared much earlier than Ediacara megafossils. This assessment is further supported by the occurrence of elements of the Weng'an biota, including the multicellular alga *Wengania* and the spiny acritarch *Tianzhushania*, in chert nodules of the lower Doushantuo Formation in the Yangtze Gorges area (*c.* 632 Ma, Condon *et al.* 2005; Liu *et al.* 2014; Zhou *et al.* 2007).

Three U–Pb zircon dates from volcanic ash beds were respectively reported from the top of the cap dolostone unit (635.2 ± 0.6 Ma), the lower part (632.5 ± 0.5 Ma) and the uppermost Doushantuo Formation (551.1 ± 0.7 Ma) in the Yangtze Gorges area (Condon *et al.* 2005), which provide a direct age constraint on the termination of the Marinoan global glaciation and an approximate temporal framework for the Ediacaran fossil assemblages, including Miaohe (Xiao *et al.* 2002) and Shibantan biotas (Chen *et al.* 2013, 2014*b*). However, the direct age constraints on many other Ediacaran fossil biotas such as the Lantian biota (Yuan *et al.* 2011), and on the pronounced negative $\delta^{13}C$ excursion event (e.g. EN3, McFadden *et al.* 2008; Zhou & Xiao, 2007), a probable equivalent to the middle Ediacaran Shuram/Wonoka anomaly (Le Guerroué *et al.* 2006; Lu *et al.* 2013), are absent; this hampers our understanding of the coevolutionary pattern of Ediacaran marine organisms and environmental change, and also makes the subdivision and classification of the Ediacaran System more challenging (Xiao *et al.* 2016).

6. Conclusion

In summary, the SIMS U–Pb age of 609 ± 5 Ma from unit 5 of the Ediacaran Doushantuo Formation at Zhangcunping in Yichang, Hubei Province, provides a direct age constraint on the Weng'an biota, indicating that the Weng'an biota is much older than the macroscopic Ediacara biota. More reliable radiometric ages are needed to further elucidate both the biological and environmental evolution of Ediacaran marine ecosystems.

Acknowledgements. This work was supported by the National Basic Research Program of China (grant number 2013CB835005), the Chinese Academy of Sciences (grant number KZZD-EW-02) and the National Science Foundation (grant number EAR-1528553). We are grateful to two anonymous reviewers for their constructive suggestions.

References

Barfod, G. H., Albaréde, F., Knoll, A. H., Xiao, S., Télouk, P., Frei, R. & Baker, J. 2002. New Lu-Hf and Pb-Pb age constraints on the earliest animal fossils. *Earth and Planetary Science Letters* **201**, 203–12.

Cao, R., Tang, T., Xue, Y., Yu, C., Yin, L. & Zhao, W. 1989. Research on Sinian Strata with ore deposits in the Yangzi (Yangtze) region, China. In *Upper Precambrian of the Yangzi (Yangtze) Region, China* (ed. Nanjing Institute of Geology and Palaeontology), pp. 1–94. Nanjing: Nanjing University Press.

Chen, D., Dong, W., Zhu, B. & Chen, X. P. 2004. Pb-Pb ages of Neoproterozoic Doushantuo phosphorites in South China: Constraints on early metazoan evolution and glaciation events. *Precambrian Research* **132**, 123–32.

Chen, L., Xiao, S., Pang, K., Zhou, C. & Yuan, X. 2014a. Cell differentiation and germ-soma separation in Ediacaran animal embryo-like fossils. *Nature* **516**(7530), 238–41.

Chen, S., Yin, C., Liu, P., Gao, L., Tang, F. & Wang, Z. 2010. Microfossil assemblage from chert nodules of the Ediacaran Doushantuo Formation in Zhangcunping, northern Yichang, South China. *Acta Geologica Sinica* **84**(1), 70–7.

Chen, Y.-Q., Jiang, S.-Y., Ling, H.-F. & Yang, J.-H. 2009. Pb–Pb dating of black shales from the Lower Cambrian and Neoproterozoic strata, South China. *Chemie der Erde - Geochemistry* **69**(2), 183–9.

Chen, Z., Zhou, C., Meyer, M., Xiang, K., Schiffbauer, J. D., Yuan, X. & Xiao, S. 2013. Trace fossil evidence for Ediacaran bilaterian animals with complex behaviors. *Precambrian Research* **224**, 690–701.

Chen, Z., Zhou, C., Xiao, S., Wang, W., Guan, C., Hua, H. & Yuan, X. 2014b. New Ediacara fossils preserved in marine limestone and their ecological implications. *Scientific Reports* **4**, 4180.

Condon, D., Zhu, M., Bowring, S., Wang, W., Yang, A. & Jin, Y. 2005. U-Pb ages from the Neoproterozoic Doushantuo Formation, China. *Science* **308**, 95–8.

Ding, L., Li, Y., Hu, X., Xiao, Y., Su, C. & Huang, J. 1996. *Sinian Miaohe Biota*. Beijing: Geological Publishing House.

Grotzinger, J. P., Bowring, S. A., Saylor, B. Z. & Kaufman, A. J. 1995. Biostratigraphic and

geochronologic constraints on early animal evolution. *Science* **270**, 598–604.

Hagadorn, J. W., Xiao, S., Donoghue, P. C. J., Bengtson, S., Gostling, N. J., Pawlowska, M., Raff, E. C., Raff, R. A., Turner, F. R., Yin, C., Zhou, C., Yuan, X., McFeely, M. B., Stampanoni, M. & Nealson, K. H. 2006. Cellular and subcellular structure of Neoproterozoic animal embryos. *Science* **314**, 291–4.

Jiang, G., Shi, X., Zhang, S., Wang, Y. & Xiao, S. 2011. Stratigraphy and paleogeography of the Ediacaran Doushantuo Formation (ca. 635-551 Ma) in South China. *Gondwana Research* **19**(4), 831–49.

Knoll, A. H., Javaux, E. J., Hewitt, D. & Cohen, P. 2006. Eukaryotic organisms in Proterozoic oceans. *Philosophical Transactions of the Royal Society of London B: Biological Sciences* **361**(1470), 1023–38.

Le Guerroué, E., Allen, P. A., Cozzi, A., Etienne, J. L. & Fanning, M. 2006. 50 Myr recovery from the largest negative δ13C excursion in the Ediacaran ocean. *Terra Nova* **18**(2), 147–53.

Li, Q.-L., Li, X.-H., Liu, Y., Tang, G.-Q., Yang, J.-H. & Zhu, W.-G. 2010. Precise U-Pb and Pb-Pb dating of Phanerozoic baddeleyite by SIMS with oxygen flooding technique. *Journal of Analytical Atomic Spectrometry* **25**(7), 1107–13.

Li, X., Tang, G., Gong, B., Yang, Y., Hou, K., Hu, Z., Li, Q., Liu, Y. & Li, W. 2013. Qinghu zircon: a working reference for microbeam analysis of U-Pb age and Hf and O isotopes. *Chinese Science Bulletin* **58**(36), 4647–54.

Li, X.-H., Liu, Y., Li, Q.-L., Guo, C.-H. & Chamberlain, K. R. 2009. Precise determination of Phanerozoic zircon Pb/Pb age by multicollector SIMS without external standardization. *Geochemistry, Geophysics, Geosystems* **10**(4), doi: 10.1029/2009GC002400.

Liu, P., Chen, S., Zhu, M., Li, M., Yin, C. & Shang, X. 2014. High-resolution biostratigraphic and chemostratigraphic data from the Chenjiayuanzi section of the Doushantuo Formation in the Yangtze Gorges area, South China: Implication for subdivision and global correlation of the Ediacaran System. *Precambrian Research* **249**, 199–214.

Liu, P., Yin, C., Gao, L., Tang, F. & Chen, S. 2009. New material of microfossils from the Ediacaran Doushantuo Formation in the Zhangcunping area, Yichang, Hubei Province and its zircon SHRIMP U-Pb age. *Chinese Science Bulletin* **54**(6), 1058–64.

Liu, X., Gao, S., Diwu, C. & Ling, W. 2008. Precambrian crustal growth of Yangtze Craton as revealed by detrital zircon studies. *American Journal of Science* **308**(4), 421–68.

Lu, M., Zhu, M., Zhang, J., Shields-Zhou, G., Li, G., Zhao, F., Zhao, X. & Zhao, M. 2013. The DOUNCE event at the top of the Ediacaran Doushantuo Formation, South China: broad stratigraphic occurrence and non-diagenetic origin. *Precambrian Research* **225**(0), 86–109.

Ludwig, K. R. 2008. *Users' Manual for Isoplot 3.70: A Geochronological Toolkit for Mircrosoft Excel*. Berkeley, California: Berkeley Geochronology Center Special Publication.

Martin, M. W., Grazhdankin, D. V., Bowring, S. A., Evans, D. A. D., Fedonkin, M. A. & Kirschvink, J. L. 2000. Age of Neoproterozoic bilaterian body and trace fossils, White Sea, Russia: implications for metazoan evolution. *Science* **288**, 841–5.

Maynard Smith, J. & Szathmary, E. 1998. *The Major Transitions in Evolution*. Oxford: Oxford University Press.

McFadden, K. A., Huang, J., Chu, X., Jiang, G., Kaufman, A. J., Zhou, C., Yuan, X. & Xiao, S. 2008. Pulsed oxidation and biological evolution in the Ediacaran Doushantuo Formation. *Proceedings of the National Academy of Sciences* **105**(9), 3197–202.

McFadden, K. A., Xiao, S., Zhou, C. & Kowalewski, M. 2009. Quantitative evaluation of the biostratigraphic distribution of acanthomorphic acritarchs in the Ediacaran Doushantuo Formation in the Yangtze Gorges area, South China. *Precambrian Research* **173**(1–4), 170–90.

Narbonne, G. M. 2004. Modular construction of early Ediacaran complex life forms. *Science* **305**, 1141–4.

Sláma, J., Košler, J., Condon, D. J., Crowley, J. L., Gerdes, A., Hanchar, J. M., Horstwood, M. S. A., Morris, G. A., Nasdala, L., Norberg, N., Schaltegger, U., Schoene, B., Tubrett, M. N. & Whitehouse, M. J. 2008. Plešovice zircon – A new natural reference material for U–Pb and Hf isotopic microanalysis. *Chemical Geology* **249**(1–2), 1–35.

Stacey, J. S. & Kramers, J. D. 1975. Approximation of terrestrial lead isotope evolution by a two-stage model. *Earth and Planetary Science Letters* **26**(2), 207–21.

Wan, B., Yuan, X., Chen, Z., Guan, C., Pang, K., Tang, Q. & Xiao, S. 2016. Systematic description of putative animal fossils from the early Ediacaran Lantian Formation of South China. *Palaeontology* **59**(4), 515–32.

Wiedenbeck, M., Allé, P., Corfu, F., Griffin, W. L., Meier, M., Oberli, F., Quadt, A. V., Roddick, J. C. & Spiegel, W. 1995. Three natural zircon standards for U-Th-Pb, Lu-Hf, trace-element and REE analyses. *Geostandards Newsletter* **19**(1), 1–23.

Xiao, S. & Laflamme, M. 2008. On the eve of animal radiation: phylogeny, ecology and evolution of the Ediacara biota. *Trends in Ecology and Evolution* **24**(1), 31–40.

Xiao, S., Muscente, A., Chen, L., Zhou, C., Schiffbauer, J. D., Wood, A. D., Polys, N. F. & Yuan, X. 2014a. The Weng'an biota and the Ediacaran radiation of multicellular eukaryotes. *National Science Review* **1**, 498–520.

Xiao, S., Narbonne, G. M., Zhou, C., Laflamme, M., Grazhdankin, D. V., Moczydłowska-Vidal, M. & Cui, H. 2016. Towards an Ediacaran time scale: problems, protocols, and prospects. *Episodes*, **39**(4), 540–55.

Xiao, S., Yuan, X., Steiner, M. & Knoll, A. H. 2002. Macroscopic carbonaceous compressions in a terminal Proterozoic shale: A systematic reassessment of the Miaohe biota, South China. *Journal of Paleontology* **76**(2), 347–76.

Xiao, S., Zhang, Y. & Knoll, A. H. 1998. Three-dimensional preservation of algae and animal embryos in a Neoproterozoic phosphorite. *Nature* **391**, 553–8.

Xiao, S., Zhou, C., Liu, P., Wang, D. & Yuan, X. 2014b. Phosphatized acanthomorphic acritarchs and related microfossils from the Ediacaran Doushantuo Formation at Weng'an (South China) and their implications for biostratigraphic correlation. *Journal of Paleontology* **88**(1), 1–67.

Ye, Q., Tong, J., An, Z., Tian, L., Zhao, X. & Zhu, S. 2015. Phosphatized fossil assemblage from the Ediacaran Doushantuo Formation in Zhangcunping area, Yichang, Hubei Province. *Acta Petrologica Sinica* **54**(1), 43–65.

Yuan, X., Chen, Z., Xiao, S., Zhou, C. & Hua, H. 2011. An early Ediacaran assemblage of macroscopic

and morphologically differentiated eukaryotes. *Nature* **470**(7334), 390–93.

Yuan, X., Xiao, S., Yin, L., Knoll, A. H., Zhou, C. & Mu, X. 2002. *Doushantuo Fossils: Life on the Eve of Animal Radiation*. Hefei, China: China University of Science and Technology Press.

Zhou, C. & Xiao, S. 2007. Ediacaran $d^{13}C$ chemostratigraphy of South China. *Chemical Geology* **237**, 89–108.

Zhou, C., Xie, G., McFadden, K., Xiao, S. & Yuan, X. 2007. The diversification and extinction of Doushantuo-Pertatataka acritarchs in South China: causes and biostratigraphic significance. *Geological Journal* **42**, 229–62.

Zhou, C., Xie, G. & Xiao, S. 2005. New data of microfossils from Doushantuo Formation at Zhangcunping in Yichang, Hubei Province. *Acta Micropalaeontologica Sinica* **22**(3), 217–24.